Toxicology in Vitro 44 (2017) 100–110

Contents lists available at ScienceDirect

Toxicology in Vitro

journal homepage: www.elsevier.com/locate/toxinvit

Effects of mild ozonisation on gene expression and nuclear domains organization in vitro

C. Scassellati[a], M. Costanzo[b], B. Cisterna[b], A. Nodari[b], M. Galiè[b], A. Cattaneo[c,d], V. Covi[e], G. Tabaracci[e], C. Bonvicini[a,1], M. Malatesta[b,*,1]

[a] Genetics Unit, IRCCS San Giovanni di Dio - Fatebenefratelli, Brescia, Italy
[b] Department of Neurosciences, Biomedicine and Movement Sciences, Anatomy and Histology Section, University of Verona, Italy
[c] Biological Psychiatry Unit, IRCCS San Giovanni di Dio - Fatebenefratelli, Brescia, Italy
[d] Stress, Psychiatry and Immunology Laboratory, Department of Psychological Medicine, Institute of Psychiatry, King's College London, London, UK
[e] San Rocco Clinic, Montichiari, (BS), Italy

ARTICLE INFO

Keywords:
Ozone
Human neuroblastoma cells
Cell nucleus
Transmission electron microscopy
Whole gene expression

ABSTRACT

In the last two decades, the use of ozone (O_3) as a complementary medical approach has progressively been increasing; however, its application is still limited due to the numerous doubts about its possible toxicity, despite the low concentrations used in therapy. For an appropriate and safe clinical application of a potentially toxic agent such as O_3, it is crucial to elucidate the cellular response to its administration. Molecular analyses and transmission electron microscopy were here combined to investigate in vitro the effects of O_3 administration on transcriptional activity and nuclear domains organization of cultured SH-SY5Y neuronal cells; low O_3 concentrations were used as those currently administered in clinical practice. Mild ozonisation did not affect cell proliferation or death, while molecular analyses showed an O_3-induced modulation of some genes involved in the cell response to stress (*HMOX1*, *ERCC4*, *CDKN1A*) and in the transcription machinery (*CTDSP1*). Ultrastructural cytochemistry after experiments of bromouridine incorporation consistently demonstrated an increased transcriptional rate at both the nucleoplasmic (mRNA) and the nucleolar (rRNA) level. No ultrastructural alteration of nuclear domains was observed.

Our molecular, ultrastructural and cytochemical data demonstrate that a mild toxic stimulus such as mild ozonisation stimulate cell protective pathways and nuclear transcription, without altering cell viability. This could possibly account for the positive effects observed in ozone-treated patients.

1. Introduction

Ozone (O_3) is a highly unstable atmospheric gas that rapidly decomposes to normal oxygen (O_2). Although not being a radical molecule, O_3 is a very strong oxidant and, due to this highly toxic property, it has been widely used as a disinfectant agent, also for medical purposes (Travagli et al., 2010; Davies et al., 2011; Gupta and Mansi, 2012). In addition to its germicidal application, O_3 administration as O_2-O_3 gas mixture has proven to exert therapeutic effects in numerous diseases, including arthritis, heart and vascular diseases, asthma, emphysema, and multiple sclerosis (reviews in Re et al., 2008; Elvis and Ekta, 2011; Bocci, 2012). In the last two decades, the use of O_3 as a complementary medical approach has progressively been increasing all over the world; low O_3 concentrations are generally used in the medical practice but the application of O_3 therapy is still limited due to the numerous doubts about its possible toxicity. Knowledge of the cellular response to O_3 administration is therefore crucial for its appropriate and safe clinical application.

It has been hypothesized that exposure to mild O_3 concentrations may stimulate the cellular antioxidant defenses without inducing cell damage (Sagai and Bocci, 2011). Unfortunately, scientific data demonstrating activation of cytoprotective pathways are still scarce and inconclusive (Re et al., 2014; Güçlü et al., 2016).

To elucidate this point, we investigated the effects of low O_3

Abbreviations: SH-SY5Y, Human neuroblastoma cell line; *HMOX1*, Heme Oxygenase 1; *ERCC4*, Excision Repair Cross-Complementation Group 4; *CDKN1A*, Cyclin-Dependent Kinase Inhibitor 1A; *CTDSP1*, CTD Small Phosphatase 1

* Corresponding author at: Department of Neurosciences, Biomedicine and Movement Sciences, Anatomy and Histology Section, University of Verona, Strada Le Grazie 8, I-37134 Verona, Italy.
E-mail address: manuela.malatesta@univr.it (M. Malatesta).
[1] Co-last authorship.

http://dx.doi.org/10.1016/j.tiv.2017.06.021
Received 22 January 2017; Received in revised form 15 June 2017; Accepted 22 June 2017
Available online 23 June 2017
0887-2333/

concentrations currently used in clinical practice on the nuclear activity of cultured cells of neuronal origin. There is, in fact, a growing interest for therapeutic applications of O_3 to the nervous system based on experimental evidence that mild ozonisation induces metabolic stimulation and even regenerative effects in neurons (Molinari et al., 2014; Salem et al., 2016; Tural Emon et al., 2016; Ozbay et al., 2017). The use of an in vitro model ensured controlled experimental conditions, allowing analysis of the direct effects of mild ozonisation on nuclear function without the intermediation of blood/tissue factors as occurs in vivo. Moreover, the choice of a stabilised neuroblastoma cell line, characterized by negligible intersample variability compared to primary cell cultures, guaranteed the consistency of our experimental model with highly sensitive techniques such as genomic and ultrastructural analysis. The combination of molecular assays (microarray gene expression and Real Time qPCR) and microscopy techniques (transmission electron microscopy and ultrastructural immunocytochemistry) allowed investigation of the effects of O_3 exposure on gene expression and the organization of nuclear domains.

2. Materials and methods

2.1. Cell culture and ozone treatment

SH-SY5Y cells (a human neuroblastoma cell line) (5×10^5) were seeded on 75 cm^2 plastic flasks (Corning Inc., Corning, NY, USA) in a 1:1 mixture of EMEM (Eagle's Minimum Essential Medium) and F12 medium supplemented with 10% (v/v) fetal bovine serum, 1% (w/v) NEAA (Non-Essential Amino Acids Solution), 0.5% (w/v) glutamine, 100 U of penicillin and 100 μg/ml streptomycin (Gibco by Life Technologies), at 37 °C in a 5% CO_2 humidified atmosphere. When subconfluent, the cells were mildly trypsinized (0.25% trypsin containing 0.05% ethylene diamino tetraacetic acid (EDTA) in phosphate-buffered saline, PBS) and exposed in suspension to O_2-O_3 gas mixtures with two O_3 concentrations successfully used for therapeutic purposes (10 and 16 μg O_3/ml O_2). A high concentration (100 μg O_3/ml O_2) was also used as a control for a strong oxidative stress. The gas was produced by an OZO2 FUTURA apparatus (Alnitec s.r.l., Cremosano, CR, Italy), which generates O_3 from medical-grade O_2, and allows photometric real-time control of gas flow rate and O_3 concentration. The reliability of the experimental procedure was guaranteed by choosing a well-established technique for cell ozonisation (Larini et al., 2003), which ensures that a defined number of cells are exposed to an exact gas volume at a pressure corresponding to the atmospheric one, and that the cell sample reacts totally with the O_3 dose for a precise treatment time. Briefly, for each sample, 4×10^5 cells were suspended in 1 ml medium into a 10 ml syringe (Terumo Medical Corporation, Somerset, NJ, USA), an equal volume of gas was then collected in the syringe, and the sample was gently mixed with the gas for 10 min to allow cells to react with the O_3.

Cells exposed to pure O_2 under the same experimental conditions were used to discriminate the effect of O_3, while cells exposed to air served as control (CTR).

Three hours after the exposure to the different gases or air, the cells were processed for genomic or microscopy analyses, while other samples were allowed to grow for 24 h and 48 h, to estimate the effect of O_3 on cell viability and proliferation (see below). For Western blot analysis, the cells were processed 10 min after treatment.

2.2. Cell viability and proliferation

To determine the effect of gas exposure on cell survival and growth, 5×10^4 cells/well were seeded on 6 multiwell plastic microplates (Corning), and the fraction of dead cells was estimated 3 h after treatment, whereas the total cell number was assessed after 24 h and 48 h. The cells were detached by mild trypsinization as above, stained for 2 min with 0.1% trypan blue in the culture medium, and scored in a Burker hemocytometer using a Leica DM IL inverted microscope equipped with 10 × objective lens. Data were expressed as the mean of three independent experiments ± standard error of the mean (SE).

Results for each measured variable were pooled according to the experimental group and the mean ± SE value calculated. Statistical comparisons were performed by the one way-Anova test and post-hoc pairwise comparisons.

2.3. RNA isolation and microarray gene expression analyses

Three hours after gas exposure, RNA samples were extracted and purified from the cells by using the RNeasy Mini kit (Qiagen, Hilden, Germany) according to the manufacturer's protocols. The concentration of total RNA was quantified using the Nanodrop 2000 (Nanodrop Technologies, Wilmington, DE, USA) by measuring the absorbance at 260 nm. Additionally, the OD260/230 and OD260/280 ratios were determined to assess RNA purity. RNA integrity was assessed with the 2100 Bioanalyzer (Agilent Technology, Santa Clara, CA, USA) using an RNA 6000 NanoChip and expressed as RNA Integrity Number (RIN), which was considered acceptable within the range of 7–10.

RNA samples from cells treated with O_2, 10 or 16 μg O_3/ml O_2 as well as the CTR were processed for transcriptomic analyses. Total RNA (250 ng) from each sample were reverse-transcribed with the Ambion WT Expression Kit (Invitrogen-Life Technologies, Carlsbad, CA, USA). Subsequently, 5.5 μg of sscDNA was fragmented and labelled with biotin. The labelled samples were hybridized onto Human Gene 1.1 ST Array Strips (Affymetrix, Inc., Santa Clara, CA, USA), comprising > 750,000 probes and representing > 28,000 genes mapped through UniGene or via RefSeq.

The reactions of hybridization, fluidics, and imaging were performed on the Affymetrix Gene Atlas instrument according to the manufacturer's instructions (http://www.affymetrix.com/support/technical/manuals.affx).

The descriptive features for each identified gene were obtained from http://www.genecards.org.

2.4. Microarray data analysis and pathway analysis

Affymetrix CEL files were imported into Partek Genomics Suite version 6.6 for data visualization and statistical testing. Quality control assessment was performed using Partek Genomic Suite 6.6. All the samples passed the quality criteria for hybridization controls, labelling controls and 3′/5′ Metrics. Background correction was conducted using Robust Multi-strip Average (RMA) (Irizarry et al., 2003) to remove noise from autofluorescence. After background correction, normalization was made using Quantiles Normalization (Bolstad et al., 2003) to normalize the distribution of probe intensities among different microarray chips. Subsequently, a summarization step was conducted using a linear median polish algorithm (Tukey, 1977) to integrate probe intensities in order to compute the expression levels for each gene transcript. Upon data upload, pre-processing of CEL data for the complete data set was performed using the Robust MultiChip Average ANOVA statistical test to assess treatment effects. Differential gene expression was assessed by applying a p-value filter (for attribute = -treatment) of $p < 0.05$ to the ANOVA results. Contrast analyses were then performed to get the following four comparisons: 10 μg O_3/ml vs CTR, 16 μg O_3/ml vs CTR, 10 μg O_3/ml vs O_2, 16 μg O_3/ml vs O_2. In this comparison, a maximum filter of $p < 0.05$ and a minimum absolute fold change cut-off of 1.2 were applied.

In order to identify common or specific genes modulated by each treatment condition, the gene lists were compared by an interactive tool Venny (Venny 2.0.2 http://bioinfogp.cnb.csic.es/tools/venny/index.html). DAVID software was used to identify molecular signalling pathways in each treatment conditions.

2.5. Reverse transcription, RT-qPCR confirmation and statistical analysis

One microgram of total RNA was used for cDNA synthesis with random hexamer primers (Invitrogen-Life Technologies) and Superscript II Reverse Transcriptase (Invitrogen-Life Technologies). The expression levels of specific transcripts in SH-SY5Y were determined by RT-qPCR using the StepOnePlus instrument (Applied Biosystems, Foster City, CA, USA) with the TaqMan assay (Applied Biosystems). The genes were analyzed and normalized to the levels of the three housekeeping (HK) genes: *GAPDH* (glyceraldehyde-3-phosphate dehydrogenase, Hs04420697_g1), *HPRT1* (hypoxanthine phosphoribosyl-transferase 1, Hs99999909_m1) and *UBC* (ubiquitin C, Hs00824723_m1). These three HK genes have been chosen according to the evidence supporting that these are the best HK genes for neuroblastoma cell lines (Vandesompele et al., 2002). Each sample was assayed in duplicate. Data analyses were performed using the comparative Ct method (also known as the $2-\Delta\Delta Ct$ method) (Schmittgen and Livak, 2008). The differential expression analysis was performed by applying generalized linear model. For multiple comparisons, the Sidak correction was applied. SPSS vs23 was used.

2.6. Western blot analysis

NRF2, a transcription factor controlling the expression of genes coding for antioxidant and cytoprotective proteins (Brigelius-Flohe and Flohe, 2011), was evaluated as an index of cellular response to the O_3 oxidant activity. SH-SY5Y cells treated with O_2, or with 10, 16 or 100 μg O_3/ml O_2, as well as CTR samples were processed for Western blot analysis. Due to the short protein half-life (Khalil et al., 2015), cell samples were analyzed 10 min after gas exposure. Immunoblots were performed according to standard procedures in RIPA buffer (150 mM NaCl, 10 mM Tris pH 7.5, 1% NP40, 1% Deoxycholate, 0.1% SDS) supplemented with phosphatase and protease inhibitors (Sigma, St. Louis, MO, USA). Samples were resolved on Tris-glicine 4–20% gradient SDS-PAGE (Bio-Rad, Hercules, CA, USA), blotted on Protran® membrane 0.2 μm (Whatman®) and developed with ECL (Amersham®). The following antibodies were used: anti-NF-E2-related factor-2 (NRF2) [EP1808Y] (Abcam, Cambridge, UK, #ab62352); anti-Phospho-NRF2^{Ser40} [EP1809Y] (Abcam #76026); β − Actin (Sigma).

2.7. Transmission electron microscopy

Morphological, morphometric and cytochemical analyses were carried out at transmission electron microscopy, in order to analyse the effects of exposure to low O_3 concentrations on the fine nuclear features. The intranuclear distribution of the nuclear structural constituents involved in RNA transcription and maturation is, in fact, spatially ordered and, whenever RNA processing is altered, their organization, molecular composition, and intranuclear location are also affected (e.g., Lafarga et al., 1993; Puvion and Puvion-Dutilleul, 1996; Biggiogera et al., 2008; Malatesta et al., 2010).

SH-SY5Y cells from three independent experiments were seeded on glass coverslips placed in 6 multiwell plastic microplates (Corning) and then processed for transmission electron microscopy 3 h after gas exposure: they were fixed with 4% paraformaldehyde in 0.1 M Sörensen phosphate buffer at 4 °C for 1 h, washed, treated with 0.5 M NH_4Cl in PBS, dehydrated with ethanol and embedded in LRWhite resin. To evaluate RNA transcription rate, before fixation the cells were pulse-labelled with 10 mM 5-bromouridine (BrU, Sigma-Aldrich) for 10 min at 37 °C.

To investigate the ultrastructural morphology, some ultrathin sections were conventionally stained with lead citrate. A morphometric analysis was also carried out in 20 nucleoli (× 18,000) per sample by evaluating the total area and the percentage of area occupied by the nucleolar components: fibrillar centres (where rDNA is located (Biggiogera et al., 2001; Cisterna and Biggiogera, 2010)), dense fibrillar component (where transcription and early splicing of pre-rRNA occur (Biggiogera et al., 2001; Cmarko et al., 2000)), and granular component (where pre-ribosomes are stored (Cisterna and Biggiogera, 2010)). The ultrastructural morphometric evaluation of the relative amounts of nucleolar components is, in fact, a well-established method to get information on nucleolar activity (Schwarzacher and Wachtler, 1993).

Other ultrathin sections were processed for immunocytochemistry as described in Costanzo et al. (2015). The anti-BrdU mouse monoclonal antibody (BD Biosciences, Franklin Lakes, NJ, USA), which cross-reacts with BrU (Jensen et al., 1993), was used to identify the BrU molecules incorporated into the newly transcribed RNAs; the immunopositivity was revealed with a specific secondary 12 nm gold-conjugated antibody (Jackson Immuno Research Laboratories, West Grove, PA, USA). The samples were stained according to the EDTA technique that enhances the contrast of ribonucleoprotein-containing nuclear components, involved in RNA transcription and splicing (Bernhard, 1969): namely, the fine fibrillar structures (named perichromatin fibrils) and the roundish structures (named perichromatin granules), which both occur at the edge of heterochromatin clumps, and the small clustered granules (named interchromatin granules), occurring in the interchromatin space.

Quantitative assessment of the immunolabelling for BrU was carried out by estimating the gold particle density (number of gold particle/μm^2) over nucleoplasmic and nucleolar areas on 20 randomly selected nuclei (× 28,000) per sample (for technical details see Costanzo et al., 2015). For background evaluation, samples processed in the absence of the primary antibody were considered. This long-established technique (e.g. Hayat, 1992; Gingras and Bendayan, 1994; Cmarko et al., 1999, 2000; Malatesta et al., 2010) allows quantitative evaluation and statistical comparisons of the surface density of immunogold labelling in precise subcellular domains, thus simultaneously providing molecular and structural information. The same samples were used for quantitative evaluations of the nuclear structural constituents involved in mRNA processing that are visible only after EDTA staining: the size of the interchromatin granule cluster and the nucleoplasmic density of perichromatin granules (number of granules/μm^2) were estimated.

Results for each measured variable were pooled according to the experimental group and the mean ± SE value calculated. Statistical comparisons were performed by the one way-Anova test and post-hoc pairwise comparisons.

All samples were observed in a Philips Morgagni transmission electron microscope (FEI Company Italia Srl, Milan, Italy) operating at 80 kV and equipped with a Megaview II camera (FEI Company Italia Srl, Milan, Italy) for digital image acquisition.

3. Results

3.1. Cell viability and proliferation

The trypan blue exclusion test demonstrated that the percentage of dead cells was similar in cells exposed to air, O_2, 10 μg O_3/ml and 16 μg O_3/ml, remaining below 4% (Fig. 1a). In O_3 100 μg/ml-treated samples the percentage of dead cells was significantly raised compared to all groups.

The number of cells was similar in control and low O_3 concentration-treated samples, after both 24 h and 48 h (Fig. 1b), which indicates that no effect on cell proliferation was induced by mild ozonisation.

3.2. Microarray gene expression analyses

To identify genes modulated by the two low concentrations of O_3 used, microarray gene expression analyses were performed. We found 70 modulated genes after the comparisons between 10 μg O_3/ml O_2 vs CTR, 58 genes after 16 μg O_3/ml O_2 vs CTR, 27 genes after 10 μg O_3/ml O_2 vs O_2 samples, and 42 genes after 16 μg O_3/ml O_2 vs O_2.

In order to identify common or specific genes modulated by these

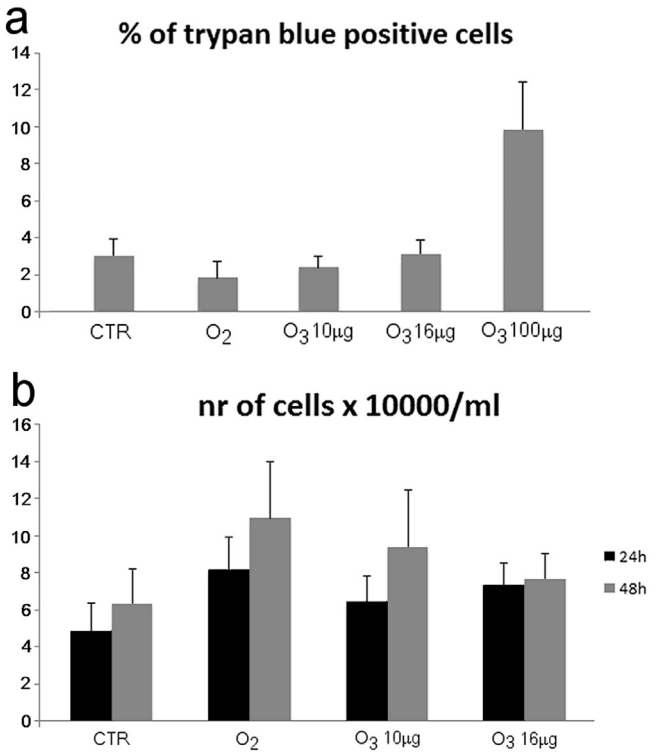

Fig. 1. Effect of O_3 exposure on cell death and proliferation. a) Mean values ± SE of dead cell percentage evaluated by trypan blue staining at 3 h post-ozonisation. The values of O_3 100 µg/ml-treated cells are significantly higher compared to all groups ($p < 0.001$). b) Mean values ± SE of cell number 24 h and 48 h post-ozonisation. No significant difference has been found among experimental groups at the same time post-treatment.

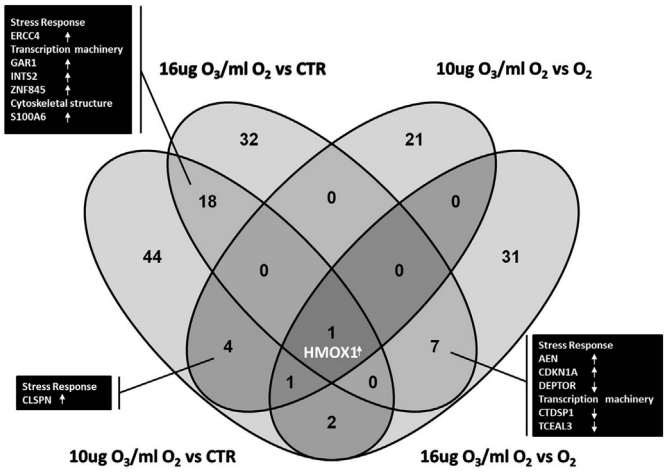

Fig. 2. Common and specific genes modulated by different treatment conditions obtained by using the interactive tool Venny. 18 modulated common genes were obtained after the comparisons between 10 µg O_3/ml vs CTR and 16 µg O_3/ml vs CTR. Of these 18 genes, 6, all up-regulated (arrows), are involved in pathways potentially linked to O_3 action mechanism: *ERCC4* (stress response), *GAR1*, *INTS2*, *ZNF845* (transcription machinery), *S100A6* (cytoskeletal structure). Seven modulated common genes were obtained after the comparisons between 16 µg O_3/ml vs CTR and 16 µg O_3/ml vs O_2. Of these 7 genes, 5 belong to pathways potentially linked to O_3 action mechanism: *AEN*, *CDKN1A* (both up-regulated, arrows) and *DEPTOR* (down-regulated, arrow) are involved in stress response, *CTDSP1* and *TCEAL3* (both down-regulated, arrows) are involved in transcription machinery. Finally, 4 modulated common genes were obtained after the comparisons 10 µg O_3/ml vs CTR and 10 µg O_3/ml vs O_2. Of these 4 genes, *CLSPN* (up-regulated, arrow) is involved in stress response. One gene resulted up-regulated after all comparisons, *HMOX1* resulted up-regulated after the comparisons between 16 µg O_3/ml vs O_2 and 10 µg O_3/ml vs O_2.
ERCC4 = Excision Repair Cross-Complementation Group 4; *GAR1* = GAR1 Ribonucleoprotein; *INTS2* = Integrator Complex Subunit 2; *ZNF845* = Zinc Finger Protein 845; *S100A6* = S100 Calcium Binding Protein A6; *HMOX1* = Heme Oxygenase (Decycling) 1; *AEN* = Apoptosis Enhancing Nuclease; *CDKN1A* = Cyclin-Dependent Kinase Inhibitor 1A (P21, Cip1); *DEPTOR* = DEP Domain Containing MTOR-Interacting Protein; *CTDSP1* = CTD (Carboxy-Terminal Domain, RNA Polymerase II, Polypeptide A) Small Phosphatase 1; *TCEAL3* = Transcription Elongation Factor A (SII)-Like 3; *CLSPN* = claspin.

treatment conditions, the equivalent gene lists were compared by using an interactive tool Venny (Fig. 2). In particular, we focused on those genes in common between the different comparisons. The results indicated that 18 modulated genes were obtained after the comparisons between 10 µg O_3/ml O_2 vs CTR and 16 µg O_3/ml O_2 vs CTR (Table 1). Two of these genes (Heterogeneous Nuclear Ribonucleoprotein C-Like 1, *HNRPCL1*, and Chromosome 3 Open Reading Frame 62, *C3orf62*) were down-regulated, while 16 genes were up-regulated (Exocyst Complex Component 5, *EXOC5*; Transmembrane Protein 242, TMEM242 and 79, *TMEM79*; Ankyrin Repeat and SOCS Box Containing 3, *ASB3*; TRNA Methyltransferase 1 Homolog (*S. cerevisiae*)-Like, *TRMT1L*; S100 Calcium Binding Protein A6, *S100A6*; Dermatan Sulfate Epimerase-Like, *DSEL*; Zinc Finger Protein 286A, *ZNF286A*; GAR1 Ribonucleoprotein, *GAR1*; Excision Repair Cross-Complementation Group 4, *ERCC4*; Sep (O-Phosphoserine) TRNA:Sec (Selenocysteine) TRNA Synthase, *SEPSECS*; Catenin (Cadherin-Associated Protein), Alpha-Like 1, *CTNNAL1*; Integrator Complex Subunit 2, *INTS2*; Zinc Finger Protein 845, *ZNF845*; Solute Carrier Family 7, Member 11, *SLC7A11*). Moreover, we identified the gene Heme Oxygenase (Decycling) 1, *HMOX1* that was up-regulated in all the O_3-treated samples compared to O_2-treated or CTR samples. Among all these genes, two are involved in stress response (*ERCC4* and *HMOX1*, up-regulated), three belong to the transcription machinery (*GAR1*, *INTS2*, *ZNF845*, all up-regulated), and one (*S100A6*, up-regulated) is implicated in cytoskeletal structuring (Fig. 2).

Furthermore, the comparisons between 16 µg O_3/ml O_2 vs CTR and 16 µg O_3/ml O_2 vs O_2 showed 7 commonly modulated genes (Table 1). Three of these genes are involved in stress response: Apoptosis Enhancing Nuclease, *AEN*, Cyclin-Dependent Kinase Inhibitor 1A (P21, Cip1), *CDKN1A* (both up-regulated) and DEP Domain Containing MTOR-Interacting Protein, *DEPTOR* (down-regulated). Two other genes belong to the transcription machinery: CTD (Carboxy-Terminal Domain, RNA Polymerase II, Polypeptide A) Small Phosphatase 1, *CTDSP1* and (Transcription Elongation Factor A (SII)-Like 3), *TCEAL3* (both down-regulated) (Fig. 2). The comparisons between 10 µg O_3/ml O_2 vs CTR and 10 µg O_3/ml O_2 vs O_2 showed 4 commonly modulated genes (Table 1); one of them - claspin *CLSPN* gene (up-regulated) - is involved in stress response (Fig. 2).

In addition, we performed pathway analyses on all genes modulated by O_3 both at 10 or 16 µg O_3/ml O_2 vs CTR or O_2. The results showed that the only pathway in common among the four comparisons performed was the signalling associated to *HMOX-1*.

3.3. RT-qPCR validation

Among the genes found as significantly modulated from the microarrays data, we selected for validation in Real Time PCR (RT-qPCR) those that were modulated by O_3-O_2 treatment and involved in stress response and transcription machinery: *HMOX1* (Hs01110251_m1), *ERCC4* (Hs01063530_m1), *GAR1* (Hs00852376_g1), *INTS2* (Hs01125681_g1), *ZNF845* (Hs00874661_g1), *S100A6* (Hs01002197_g1), *CLSPN* (Hs00898642_g1), *AEN* (Hs00901422_m1), *CDKN1A* (Hs00355782_m1), *DEPTOR* (Hs00224437_m1), *CTDSP1* (Hs01105503_m1), *TCEAL3* (Hs03056487_g1). The data obtained from these genes were compared with CTR, O_2, 10 µg O_3/ml O_2, 16 µg O_3/ml O_2 and 100 µg O_3/ml O_2. We considered significant after Sidak correction the data resulting from all three HK genes. The findings, shown in Table 2, confirmed modifications in the mRNA levels of *ERCC4* (100 µg O_3/ml O_2 vs CTR and O_2); *CDKN1A* (16/100 µg O_3/ml O_2 vs CTR and O_2); *CTDSP1* (16 µg O_3/ml O_2 vs CTR and O_2)

Table 1
Common genes modulated by different treatment conditions. 18 modulated genes were obtained after the comparisons between 10 μg O_3/ml vs CTR and 16 μg O_3/ml vs CTR. Seven modulated genes were obtained after the comparisons between 16 μg O_3/ml vs CTR and 16 μg O_3/ml vs O_2. Four modulated genes were obtained after the comparisons 10 μg O_3/ml vs CTR and 10 μg O_3/ml vs O_2. HMOX1 is a gene in common between the all comparisons. Each gene is linked to the respective p value and fold-change.

Gene symbol	Ref seq	Chromosome	Gene_assignment	Description	p-Value	Fold-change	Description	p-Value	Fold-change
HNRNPCL1	BC137258	1p36.21	Heterogeneous nuclear ribonucleoprotein C-like 1	10 μg O_3/ml vs CTR	0.0329	−1.33	16 μg O_3/ml vs CTR	0.0402	−1.31
C3orf62	AK096799	3p21.31	Chromosome 3 open reading frame 62	10 μg O_3/ml vs CTR	0.0032	−1.29	16 μg O_3/ml vs CTR	0.0029	−1.30
EXOC5	AK295085	14q22.3	Exocyst complex component5	10 μg O_3/ml vs CTR	0.0289	1.20	16 μg O_3/ml vs CTR	0.0168	1.23
TMEM242	BC029130	6q25.3	Trans membrane protein 242	10 μg O_3/ml vs CTR	0.0079	1.22	16 μg O_3/ml vs CTR	0.0008	1.35
TMEM79	AK056816	1q22	Trans membrane protein 79	10 μg O_3/ml vs CTR	0.0074	1.22	16 μg O_3/ml vs CTR	0.0009	1.33
ASB3	BC009569	2p16-p14	Ankyrin repeat and SOCS box containing 3	10 μg O_3/ml vs CTR	0.0338	1.24	16 μg O_3/ml vs CTR	0.0444	1.22
TRMT1L	AF288399	1q25.2	tRNA methyltransferase 1 homolog (*S. cerevisiae*)-like	10 μg O_3/ml vs CTR	0.0329	1.2	16 μg O_3/ml vs CTR	0.0284	1.24
S100A6	BC009017	1q21	S100 calcium binding protein A6	10 μg O_3/ml vs CTR	0.0442	1.24	16 μg O_3/ml vs CTR	0.0088	1.36
DSEL	AF480435	18q22.1	Dermatan sulfate epimerase-like	10 μg O_3/ml vs CTR	0.0004	1.26	16 μg O_3/ml vs CTR	0.0001	1.31
ZNF286A	AF217226	17p11.2	Zinc finger protein 286°	10 μg O_3/ml vs CTR	0.0121	1.27	16 μg O_3/ml vs CTR	0.0265	1.22
HMOX1	BC001491	22q13.1	Heme oxygenase (decycling) 1	10 μg O_3/ml vs CTR	0.0110	1.28	16 μg O_3/ml vs CTR	0.0070	1.31
GAR1	BC003413	4q25	GAR1 ribonucleoprotein homolog (yeast)	10 μg O_3/ml vs CTR	0.0106	1.31	16 μg O_3/ml vs CTR	0.0184	1.27
ERCC4	AK289726	16p13.12	Excision repair cross-complementing rodent repair deficiency, comp	10 μg O_3/ml vs CTR	0.0321	1.31	16 μg O_3/ml vs CTR	0.0234	1.34
SEPSECS	AF282065	4p15.2	Sep (O-phosphoserine) tRNA:Sec (selenocysteine) tRNA synthase	10 μg O_3/ml vs CTR	0.0140	1.32	16 μg O_3/ml vs CTR	0.0250	1.28
CTNNAL1	AK022834	9q31.2	Catenin (cadherin-associated protein), alpha-like 1	10 μg O_3/ml vs CTR	0.0012	1.32	16 μg O_3/ml vs CTR	0.0044	1.25
INTS2	AK299032	17q23.2	Integrator complex subunit 2	10 μg O_3/ml vs CTR	0.0030	1.34	16 μg O_3/ml vs CTR	0.0044	1.32
ZNF845	AK295079	19q13.42	Zinc finger protein 845	10 μg O_3/ml vs CTR	0.0267	1.39	16 μg O_3/ml vs CTR	0.0316	1.38
ANGPTL4	AF202636	19p13.3	angiopoietin-like 4	10 μg O_3/ml vs CTR	0.0318	1.41	16 μg O_3/ml vs CTR	0.0465	1.37
SLC7A11	AF252872	4q28.3	Solute carrier family 7(anionicaminoacidtransporterlightchain,xc-system), member 11	10 μg O_3/ml vs CTR	0.0145	1.65	16 μg O_3/ml vs CTR	0.0341	1.51
TOP3A	BC051748	17p12-p11.2	Topoisomerase (DNA) III alpha	10 μg O_3/ml vs O_2	0.0242	1.24			
HMOX1	BC001491	22q13.1	Heme oxygenase (decycling) 1	10 μg O_3/ml vs O_2	0.0187	1.25	16 μg O_3/ml vs O_2	0.0117	1.27
CSPP1	AJ583433	8q13.2	Centrosome and spindle pole associated protein 1	10 μg O_3/ml vs O_2	0.0140	1.26	16 μg O_3/ml vs O_2	0.0247	1.23
SLC41A2	BC036734	12q23.3	Solute carrier family 41, member 2	10 μg O_3/ml vs O_2	0.0096	1.28			
CLSPN	AF297866	1p34.2	claspin	10 μg O_3/ml vs O_2	0.0268	1.29			
ZP3	BC113949	7q11.23	Zona pellucida glycoprotein 3(sperm receptor)	10 μg O_3/ml vs O_2	0.0009	1.29			
DEPTOR	BC024746	8q24.12	DEP domain containing MTOR-interacting protein				16 μg O_3/ml vs O_2	0.0120	−1.39
CTDSP1	AF229162	2q35	CTD (carboxy-terminal domain, RNA polymerase II,polypeptideA) Small Phosphatase 1				16 μg O_3/ml vs O_2	0.0087	−1.28
TCEAL3	BC008703	Xq22.2	Transcription elongation factor A(SII)-like 3				16 μg O_3/ml vs O_2	0.0141	−1.21
AEN	BC020988	15q26.1	Apoptosis enhancing nuclease				16 μg O_3/ml vs O_2	0.0133	1.25
SNORA70D	NR_033337	16q22.3	Small nucleolar RNA, H				16 μg O_3/ml vs O_2	0.0113	1.29
FAM179B	BX648723	14q21.2	Family with sequence similarity 179, member B				16 μg O_3/ml vs O_2	0.0065	1.38
CDKN1A	BC000312	6p21.2	cyclin-dependent kinase inhibitor 1A (p21,Cip1)				16 μg O_3/ml vs O_2	0.0125	1.57

Table 2
List of significant modulated genes after RT-qPCR.

Genes	HK	Groups	Comparisons vs CTR									Comparisons vs O_2								
			2^{-DDCt}	SEM	B	Err Dev	Wald 95% CI		Wald χ^2	df	p	p Sidak	2^{-DDCt}	SEM	B	Err Dev	Wald 95% CI		Wald χ^2	df	p	p Sidak
ERCC4	HPRT1								19.24	4	0.001								19.41	3	2E − 04	
		[CTR]	0.00	0.06	0.00																	
		[O2]	0.11	0.06	− 0.14	0.25	− 0.64	0.35	0.33	1	0.57	0.96	0.00	0.06	0.00							
		[O3_10]	0.49	0.01	-0.57	0.25	− 1.07	− 0.08	5.13	1	0.02	0.09	0.34	0.01	− 0.43	0.20	− 0.82	− 0.03	4.54	1	0.03	0.10
		[O3_16]	0.32	0.10	− 0.40	0.25	− 0.89	0.10	2.46	1	0.12	0.39	0.19	0.10	− 0.25	0.20	− 0.64	0.14	1.57	1	0.21	0.51
		[O3_100]	1.00	0.20	− 1.00	0.25	− 1.49	− 0.51	15.72	1	7E − 05	3E − 04	0.81	0.20	-0.86	0.20	− 1.25	− 0.46	18.24	1	2E − 05	6E − 05
	GADPH								15.85	4	0.003								13.92	3	0.003	
		[CTR]	0.00	0.07	0.00																	
		[O2]	0.05	0.05	− 0.07	0.26	-0.58	0.45	0.06	1	0.80	1.00	0.00	0.05	0.00							
		[O3_10]	0.52	0.03	-0.60	0.26	− 1.12	− 0.09	5.28	1	0.02	0.08	0.45	0.03	− 0.54	0.22	− 0.97	− 0.10	5.87	1	0.02	0.05
		[O3_16]	0.39	0.03	− 0.48	0.26	− 0.99	0.04	3.30	1	0.07	0.25	0.33	0.03	− 0.41	0.22	− 0.85	0.02	3.44	1	0.06	0.18
		[O3_100]	0.84	0.11	− 0.88	0.26	− 1.39	− 0.36	11.17	1	8E − 04	0.003	0.76	0.11	-0.81	0.22	− 1.25	− 0.38	13.41	1	3E − 04	0.001
	UBC								48.30	4	8E − 10								56.12	3	4E − 12	
		[CTR]	0.00	0.04	0.00																	
		[O2]	− 0.01	0.04	0.01	0.23	− 0.45	0.46	0.00	1	0.97	1.00	0.00	0.04	0.00							
		[O3_10]	0.28	0.01	− 0.35	0.23	− 0.81	0.10	2.31	1	0.13	0.423	0.28	0.01	− 0.36	0.20	− 0.74	0.02	3.40	1	0.07	0.18
		[O3_16]	0.32	0.01	− 0.40	0.23	− 0.85	0.06	2.90	1	0.09	0.310	0.32	0.01	− 0.40	0.20	− 0.79	-0.02	4.25	1	0.04	0.11
		[O3_100]	1.62	0.06	− 1.39	0.23	− 1.84	− 0.93	35.74	1	2E-09	9E-09	1.63	0.06	− 1.40	0.20	− 1.78	− 1.01	50.87	1	1E − 12	3E − 12
CDKN1A	HPRT1								20.93	4	3E − 04								15.57	3	0.001	
		[CTR]	0.00	0.03	0.00																	
		[O2]	0.14	0.05	− 0.19	0.30	− 0.78	0.41	0.39	1	0.53	0.95	0.00	0.05	0.00							
		[O3_10]	0.56	0.03	-0.64	0.30	− 1.23	− 0.04	4.40	1	0.04	0.14	0.36	003	− 0.45	0,26	− 0.96	0.07	2.90	1	0.09	0.24
		[O3_16]	0.87	0.08	− 0.90	0.30	− 1.50	− 0.31	8.87	1	0.003	0.01	0.64	0.08	− 0.72	0.26	− 1.23	− 0.20	7.39	1	0.01	0.02
		[O3_100]	1.04	0.18	− 1.19	0.30	− 1.78	− 0.59	15.25	1	9E − 05	4E − 04	0.79	0.10	− 1.00	0.26	− 1.51	− 0.48	14.34	1	2E − 04	5E − 04
	GADPH								25.52	4	4E − 05								21.24	3	9E − 05	
		[CTR]	0.00	0.04	0.00																	
		[O2]	0.08	0.05	-0.11	0.27	-0.65	0.43	0.16	1	0.69	0.99	0.00	0.05	0.00							
		[O3_10]	0.59	0.04	-0.67	0.27	− 1.21	− 0.13	5.93	1	0.01	0.06	0.47	0.04	− 0.56	0.23	− 1.01	− 0.11	5.89	1	0.02	0.04
		[O3_16]	0.98	0.04	− 0.99	0.27	− 1.53	− 0.45	12.89	1	3E − 04	1E − 03	0.84	0.04	-0.88	0.23	− 1.33	− 0.43	14.49	1	1E − 04	4E − 04
		[O3_100]	1.09	0.08	− 1.06	0.27	− 1.60	− 0.53	14.99	1	1E − 04	4E − 04	0.94	0.08	-0.95	0.23	− 1.41	− 0.50	17.16	1	3E − 05	1E − 04
	UBC								50.90	4	2E − 10								51.61	3	4E-11	
		[CTR]	0.00	0.01																		
		[O2]	0.03	0.04	− 0.04	0.26	− 0.55	0.48	0.02	1	0.89	1.00	0.00	0.04	0.00							
		[O3_10]	0.34	0.02	− 0.42	0.26	− 0.93	0.10	2.55	1	0.11	0.37	0.30	0.02	− 0.38	0.23	-0.83	0.06	2.86	1	0.09	0.25
		[O3_16]	0.87	0.01	-0.90	0.26	− 1.42	− 0.39	11.89	1	6E − 04	2E − 03	0.83	0.01	-0.87	0.23	− 1.31	− 0.43	14.73	1	1E − 04	4E − 04
		[O3_100]	1.98	0.02	− 1.57	0.26	− 2.09	− 1.06	35.99	1	2E − 09	8E − 09	1.90	0.02	− 1.54	0.23	− 1.98	− 1.09	46.20	1	1E − 11	3E − 11
CTDSP1	HPRT1								16.55	4	0.002								10.65	3	0.01	
		[CTR]	0.00	0.05	0.00																	
		[O2]	− 0.02	0.03	0.03	0.30	− 0.56	0.62	0.01	1	0.92	1.00	0.00	0.03	0.00							
		[O3_10]	− 0.30	0.03	0.52	0.30	− 0.07	1.11	3.00	1	0.08	0.29	− 0.29	0.03	0.49	0.31	− 0.11	1.10	2.55	1	0.11	0.30
		[O3_16]	− 0.51	0.09	1.03	0.30	0.44	1.62	11.59	1	7E − 04	0.003	− 0.50	0.09	1.00	0.31	0.39	1.60	10.45	1	0.001	0.004
		[O3_100]	− 0.36	0.20	0.64	0.30	0.05	1.23	4.48	1	0.03	0.13	− 0.34	0.20	0.61	0.31	0.00	1.22	390	1	0.05	0.14
	GADPH								13.83	4	0.008								7.68	3	0.05	
		[CTR]	0.00	0.05	0.00																	
		[O2]	− 0.07	0.01	0.11	0.31	− 0.50	0.71	0.12	1	0.73	0.99	0.00	0.01	0.00							
		[O3_10]	− 0.29	0.04	0.49	0.31	− 0.12	1.10	2.51	1	0.11	0.38	− 0.23	0.04	0.38	0.32	− 0.25	1.01	1.42	1	0.23	0.55
		[O3_16]	− 0.48	0.04	0.95	0.31	0.34	1.55	9.33	1	0.002	0.01	− 0.44	0.04	0.84	0.32	0.21	1.47	6.78	1	0.01	0.03
		[O3_100]	− 0.41	0.09	0.76	0.31	0.15	1.37	6.03	1	0.01	0.05	− 0.36	0.09	0.65	0.32	0.02	1.28	4.12	1	0.04	0.12
	UBC								15.72	4	0.003								9.35	3	0.03	
		[CTR]	0.00	0.03	0.00																	
		[O2]	− 0.12	0.01	0.18	0.31	− 0.42	0.78	0.36	1	0.55	0.96	0.00	0.01	0.00.							
		[O3_10]	− 0.40	0.02	0.74	0.31	0.14	1.34	5.90	1	0.02	0.06	− 0.32	0.02	0.56	0.32	− 0.08	1.19	2.98	1	0.08	0.23

(continued on next page)

Table 2 *(continued)*

Genes	HK	Groups	Comparisons vs CTR									Comparisons vs O_2							
			2^{-DDCt}	SEM	B	Err Dev	Wald 95% CI		Wald χ^2	df	p	p Sidak	2^{-DDCt}	SEM	B	Err Dev	Wald 95% CI		Wald χ^2	df	p	p Sidak
		[O3_16]	− 0.51	0.01	1.03	031	0.43	1.63	11.34	1	0.001	0.003	− 0.44	0.01	0.85	0.32	0.21	1.48	6.82	1	0.01	0.03
		[O3_100]	− 0.16	0.04	0.25	0.31	− 0.35	0.85	0.67	1	0.41	0.88	− 0.05	0.04	0.07	0.32	− 0.57	0.70	0.04	1	0.83	1.00
									21.73	4	2E − 04								8.43	3	0.04	
HMOX1	HPRT1	[CTR]	0.00	0.07	0.00																	
		[O2]	0.38	0.02	-0.46	0.52	− 1.48	0.55	0.80	1	0.37	0.84	0.00	0.02	0.00							
		[O3_10]	2.35	0.01	− 1.75	0.52	− 2.76	− 0.73	11.27	1	0.001	0.003	1.43	0.01	− 1.28	0.56	− 2.38	− 0.18	5.19	1	0.02	0.07
		[O3_16]	1.79	0.07	− 1.48	0.52	− 2.50	− 0.46	8.09	1	0.004	0.02	1.02	0.07	− 1.01	0.56	− 2.12	0.09	3.25	1	0.07	0.20
		[O3_100]	2.93	0.08	− 1.98	0.52	− 2.99	− 0.96	14.45	1	1E-04	0.001	1.85	0.08	− 1.51	0.56	− 2.61	− 0.41	7.23	1	0.01	0.02
									28.17	4	1E − 05								1153	3	0.01	
	GADPH	[CTR]	0.00	0.08	0.00																	
		[O2]	0.31	0.03	-0.39	0.46	− 1.28	0.51	0.71	1	0.40	0.87	0.00	0.03	0.00							
		[O3_10]	2.43	0.03	− 1.78	0.46	− 2.68	− 0.88	15.04	1	1E − 04	4E − 04	1.62	0.03	− 1.39	0.49	− 2.36	− 0.42	7.96	1	0.005	0.01
		[O3_16]	1.95	0.05	− 1.56	0.46	− 2.46	− 0.66	11.59	1	7E − 04	0.003	1.26	0.05	− 1.18	0.49	− 2.14	− 0.21	5.67	1	0.02	0.05
		[O3_100]	2.62	0.24	− 1.85	0.46	− 2.75	− 0.96	16.36	1	5E − 05	2E − 04	1.77	0.24	− 1.47	0.49	− 2.44	− 0.50	8.86	1	0.003	0.01
									30.83	4	3E − 06								14.74	3	0.002	
	UBC	[CTR]	0.00	0.05	0.00																	
		[O2]	0.24	0.04	-0.31	0.49	− 1.28	0.66	0.40	1	0.53	0.95	0.00	0.04	0.00							
		[O3_10]	1.88	0.02	− 1.53	0.49	− 2.49	− 0.56	9.58	1	0.002	0.01	1.32	0.02	− 1.22	0.54	− 2.27	− 0.16	5.10	1	0.02	0.07
		[O3_16]	1.79	0.03	− 1.48	0.49	− 2.44	− 0.51	8.98	1	0.003	0.01	1.25	0.03	− 1.17	0.54	− 2.22	− 0.11	4.70	1	0.03	0.09
		[O3_100]	4.15	0.21	− 2.36	0.49	− 3.33	− 1.40	22.98	1	2E − 06	7E − 06	3.15	0.21	− 2.05	0.54	− 3.11	− 1.00	14.54	1	1E − 04	4E − 04

and *HMOX1* (10/16/100 μg O_3/ml O_2 vs CTR and 100 μg O_3/ml O_2 vs O_2). Furthermore, the trend in gene expression after 100 μg O_3/ml O_2 treatment did not differ from that observed after mild ozonisation (10 or 16 μg O_3/ml O_2).

3.4. Western blot analysis

Multiple lines of evidence have contributed to establish the notion that mild ozonisation might induce the transcription of anti-oxidant genes, such as HMOX1, via the activation of Nuclear factor (erythroid-derived 2)-like 2 (NRF2). In line with this notion, we found in O_3-treated cells a slight but dose-dependent increase of Phospo-NRF2 (S40) fraction over total NRF2 (Fig. 3).

3.5. Transmission electron microscopy

Ultrastructural observations revealed similar morphological features of the cell nuclei in CTR, O_2-treated, 10 μg O_3/ml-treated and 16 μg O_3/ml-treated cells, at 3 h post-treatment (Fig. 4). The cell nuclei showed roundish shape with finely irregular borders and a few small heterochromatin clumps associated to the nuclear periphery and the nucleoli; each nucleus usually contained one or two nucleoli characterized by a few fibrillar centres, and abundant dense fibrillar component and granular component.

In the nucleoplasm, EDTA staining allowed the visualization of the structural constituents involved in pre-mRNA transcription and processing leading to the mature mRNAs suitable for export to the cytoplasm. Numerous perichromatin fibrils (the in situ form of transcription (Fakan, 2004), splicing (Cmarko et al., 1999) and 3′ end processing (Schul et al., 1996) of pre-mRNAs) and perichromatin granules (vectors and storage sites for already spliced pre-mRNAs (Fakan, 2004)) were distributed at the edge of heterochromatin, while clusters of interchromatin granules (where storage, assembly and phosphorylation of transcription and splicing factors take place (Bogolyubov et al., 2009)) occurred in the interchromatin space (Fig. 5). No change was found in the area of interchromatin granules clusters and the density of perichromatin granules (Fig. 5 and Table 3).

The only evident morphological differences concerned the nucleoli, which showed a rather compact arrangement in CTR and O_2-treated cells (Fig. 3a, b), whereas being more reticulated, with prominent dense fibrillar component and more numerous fibrillar centres in both samples treated with low O_3 concentrations (Fig. 4c, d). Increased percentages of the dense fibrillar component and fibrillar centres in the nucleoli of O_3-treated cells were confirmed by morphometric evaluations (Table 3).

Ultrastructural immunocytochemical analyses demonstrated that in all the cell samples (Fig. 5a, b) BrU incorporation occurred in perichromatin fibrils and the nucleolar dense fibrillar component, consistently with their role in transcription and early splicing of pre-mRNA and pre-rRNA, respectively (Fakan, 2004; Biggiogera et al., 2001; Cmarko et al., 2000). Quantitative evaluation revealed a significantly higher labelling density in both the nucleoplasm and the nucleolus of O_3-treated cells. Control samples processed in the absence of primary antibodies revealed a negligible signal (not shown).

4. Discussion

As far as we know, the present investigation is the first attempt to perform a comprehensive study on the effect of mild ozonisation on cell nuclear function, combining molecular and ultrastructural approaches. Novel information has been obtained on the multiple effects on some nuclear pathways of SH-SY5Y cells in response to the exposure to low O_3 concentrations.

Our results demonstrate that exposure of SH-SY5Y cells to 10 or 16 μg O_3/ml O_2 did not induce significant alteration of their proliferation or death rate in comparison to the CTR (air-exposed) or O_2-treated

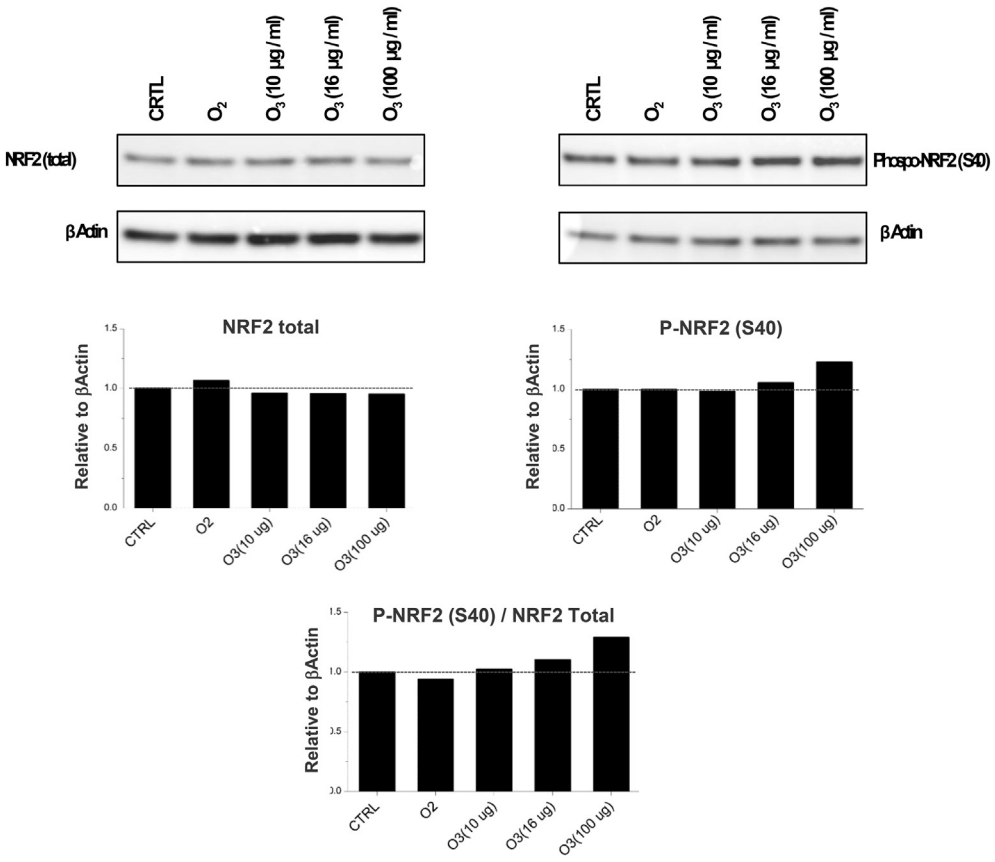

Fig. 3. Effect of O_3 exposure on NRF2 activation: O_3 exposure induced a dose-dependent increase of the fraction of NRF2 activated by the phosphorylation on Serine 40 (P-NRF2 (S40)) over the total amount of NRF2, which did not change upon treatment.

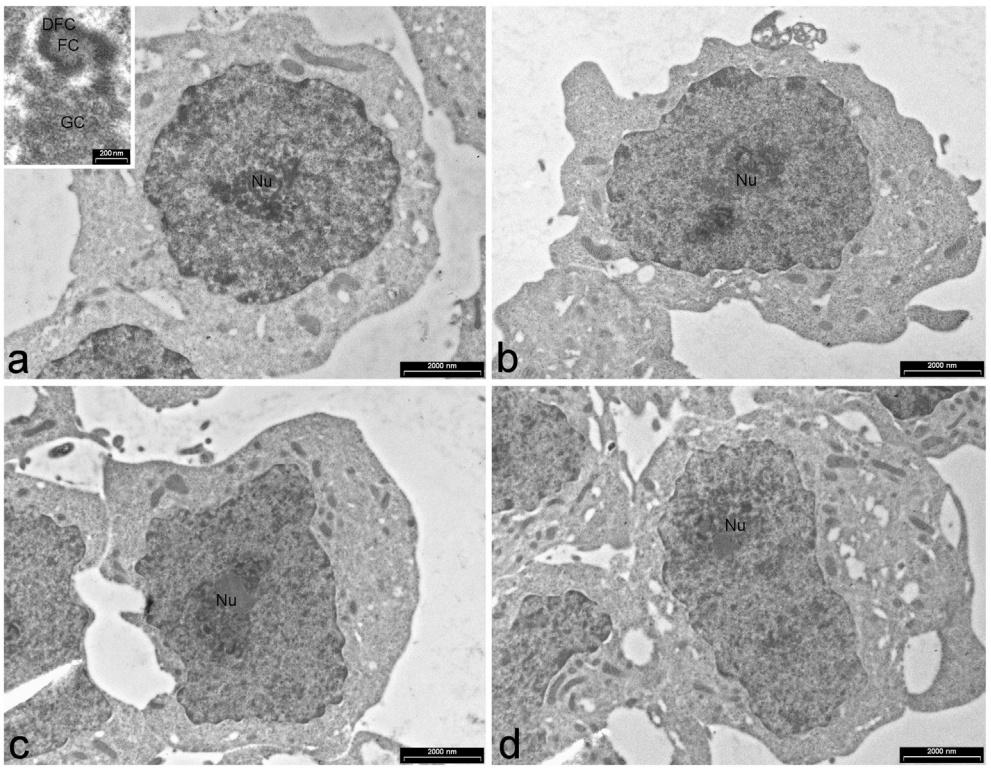

Fig. 4. Effect of O_3 exposure on nuclear ultrastructure: transmission electron micrographs of CTR (a), O_2- (b), 10 µg O_3- (c) and 16 µg O_3- (d) treated cells. Cell nuclei show similar features in all samples; however, in 10 µg and 16 µg O_3-treated cells the nucleoli (Nu) appear more reticulated than in CTR and O_2-treated cells. Inset: high magnification detail of a nucleolus showing the three structural components i.e., fibrillar center (FC), dense fibrillar component (DFC) and granular component (GC).

cells. Consistently, O_3 concentrations ranging from 1 to 20 µg/ml were found not to affect viability or proliferation of human epithelial cells in vitro (Costanzo et al., 2015). Indeed, the low O_3 concentrations used proved to affect the expression of some genes coding for proteins involved in the cytoprotective pathways (such as the regulation of DNA replication, cell cycle progression and cell death; prevention of oxidative stress damage; detoxification). Interestingly, *HMOX1*, which is upregulated in all the O_3-treated samples, codes for a protein known to

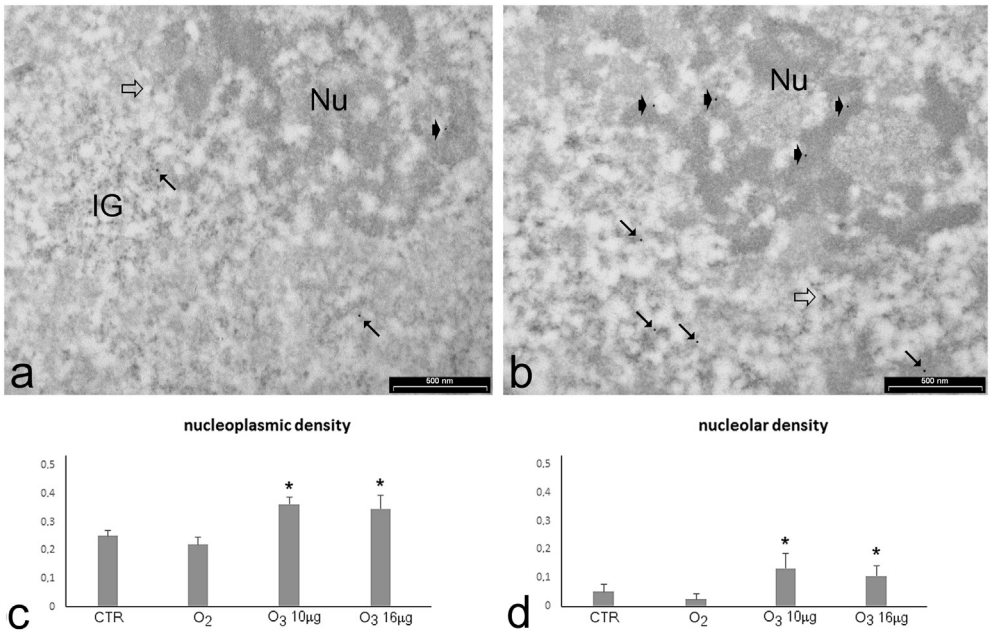

Fig. 5. Effect of O_3 exposure on RNA transcription: representative transmission electron micrographs of CTR (a) and 10 µg O_3-treated cells (b) labelled for BrU 3 h post-treatment. BrU molecules have been incorporated in perichromatin fibrils (arrows) and in the nucleolar dense fibrillar component (arrowheads). Nu, nucleolus; IG, interchromatin granules; open arrows, perichromatin granules. (c, d) Mean ± SE values of BrU labelling density evaluated on nucleoplasm and nucleoli. Asterisks indicate values significantly different from each other at the same time post-treatment.

Table 3
Means ± SD values of nucleolar variables at 3 h post-ozonisation. Values identified by asterisks are significantly different from CTR and O_2-treated samples at the same time post-treatment. IG, interchromatin granules; PG, perichromatin granules; DFC, dense fibrillar component; FC, fibrillar center; GC, granular component.

3 h post-treatment	IG cluster area (µm^2)	PG density (nr PG/µm^2)	Nucleolar area (µm^2)	% DFC	% FC	% GC
CTR cells	0.18 ± 0.10	3.12 ± 1.52	5.07 ± 3.22	31.04 ± 3.88	3.61 ± 1.32	65.00 ± 7.53
O_2-treated cells	0.16 ± 0.12	3.38 ± 1.41	4.89 ± 3.17	29.27 ± 6.64	2.99 ± 1.85	67.82 ± 8.25
10 µg O_3-treated cells	0.15 ± 0.09	3.41 ± 1.68	6.42 ± 4.01	39.68 ± 3.79*	4.88 ± 2.63*	55.65 ± 6.30*
16 µg O_3-treated cells	0.13 ± 0.08	2.84 ± 1.20	6.23 ± 3.39	38.40 ± 4.82*	4.22 ± 2.03*	57.49 ± 5.82*

protect the cell from various insults (Sun et al., 2002), while inhibiting apoptosis (Brouard et al., 2000) and promoting angiogenesis (Grochot-Przeczek et al., 2013). HMOX1 protein is also involved in modulating the activation of NRF2 (Biswas et al., 2014), which controls the expression of genes responsible for the antioxidant response (Brigelius-Flohe and Flohe, 2011). Accordingly, activation of NRF2 has been reported in peripheral blood mononuclear cells of patients submitted to ozone therapy (Re et al., 2014), as well as in our cell samples exposed to O_3. In particular, it has previously been reported that HMOX-1 up-regulation may be induced by the protein kinase C (PKC)-mediated activation of NRF2 in SH-SY5Y cells (Zhang et al., 2009; Quesada et al., 2011). NRF2 is among the major drivers of the antioxidant stress response and its activation is thought to underlie the beneficial effects of therapeutic ozonisation (Bocci and Valacchi, 2015). PKC-mediated activation of NRF2 in response to oxidative stress relies on the rapid and transitory phosphorylation of NRF2 on the serine 40 (P-NRF2 (S40)) (Huang et al., 2000). Accordingly, we found a rapid post-treatment increase of P-NRF2 (S40) fraction over the total Nrf2 protein (in accordance with the report by Khalil et al., 2015 for ovarian cancer cells).

These findings are consistent with a primary role of *HMOX1* in the cellular response following O_3 exposure. The involvement of *ERCC4* and *CDKN1A* genes (which are both up-regulated) confirms the effect of O_3 on the activation of cytoprotective pathways: in fact, *ERCC4* (belonging to the DNA nucleotide excision repair) and *CDKN1A* (playing a key role in the cellular response to stress) are both activated following DNA damage. However, the expression trend of these genes seems to be independent from the O_3 concentration: it is likely that, although an oxidative stress induces up-regulation of some key genes involved in protective pathways, the immediate cellular defence mostly relies on translational/post-translational mechanisms (such as Nrf2 phosphorylation).

Our findings support the hypothesis that a mild oxidative stress would be responsible for the activation of cytoprotective response without cell damage and, finally, for the therapeutic potential of low O_3 concentrations (Sagai and Bocci, 2011). Accordingly, there is increasing evidence that oxidative stress may not only induce deleterious damage playing a causative role in various pathogenic processes (distress), but may also act as a beneficial messenger stimulating the cell defence capacity (eustress) (recent reviews in Niki, 2016; Sies, 2017).

The O_3-induced modulation of nuclear activity takes place without any concomitant cell damage. In particular, no modification has been observed in the organization and intranuclear location of ribonucleoprotein-containing nuclear structures, demonstrating that the chronologically- and spatially-ordered RNA processing (Biggiogera et al., 2008; Malatesta et al., 2010) was not affected. In addition, our microscopy and molecular data clearly demonstrate an increased nuclear activity in O_3-treated SH-SY5Y cells. The changes in nucleolar architecture observed in O_3-treated cells are, in fact, a cytological index of nuclear activation. The nucleolus is a very dynamic structure that can rapidly adapt its activity, and consequently its structural organization, to the cell metabolic state: the enlargement of the dense fibrillar component (which is the site of rRNA synthesis and maturation) and the increase in number and size of fibrillar centres (containing rDNA) are accepted signs of increased nucleolar activity (Schwarzacher and Wachtler, 1993; Cisterna and Biggiogera, 2010). The enhanced transcriptional rate demonstrated by BrU incorporation in O_3-treated cells at both the nucleoplasmic (pre-mRNA) and nucleolar (rRNA) level represent a further evidence of metabolic activation.

5. Conclusions

Taken together, our findings demonstrate that, in our experimental

model, exposure to low O_3 concentrations stimulates cell protective pathways and nuclear transcription without altering cell proliferation and survival. More generally, our data provide structural and molecular evidence for the nuclear response activated by a mild toxic stimulus: this probably gives rise to a cascade of molecular events through multiple cellular pathways that could account for the positive effects observed in ozone-treated patients. It is worth stressing that, in our experimental system, we used the same conditions used for the administration to patients, i.e. O_3 was administered as O_3-O_2 mixture, which makes the observed effects reliably comparable to those occurring in cells in vivo.

The results of the present study may contribute to fill the current lack of evidence on the cellular mechanisms of O_3 action, thus providing a robust scientific background for its clinical application. In addition, the histochemical and molecular tests we used may also be suitable for defining protocols to test in vitro the biological effects of O_3 exposure.

Conflict of interest disclosure

The authors declare no conflict of interest.

Transparency document

The http://dx.doi.org/10.1016/j.tiv.2017.06.021 associated with this article can be found, in online version.

Acknowledgments

This work was supported by the University of Verona (Joint Projects 2015). A.N. is a PhD student in receipt of fellowships from the Doctoral Program in “Nanoscience and advanced technologies” of the University of Verona. The funding source had no involvement in study design, in the collection, analysis and interpretation of data, in the writing of the report, and in the decision to submit the paper for publication.

References

Bernhard, W., 1969. A new staining procedure for electron microscopical cytology. J. Ultrastruct. Res. 27, 250–265.
Biggiogera, M., Malatesta, M., Abolhassani-Dadras, S., Amalric, F., Rothblum, L.I., Fakan, S., 2001. Revealing the unseen: the organizer region of the nucleolus. J. Cell Sci. 114, 3199–3205.
Biggiogera, M., Cisterna, B., Spedito, A., Vecchio, L., Malatesta, M., 2008. Perichromatin fibrils as early markers of transcriptional alterations. Differentiation 76, 57–65.
Biswas, C., Shah, N., Muthu, M., La, P., Fernando, A.P., Sengupta, S., Yang, G., Dennery, P.A., 2014. Nuclear heme oxygenase-1 (HO-1) modulates subcellular distribution and activation of Nrf2, impacting metabolic and anti-oxidant defenses. J. Biol. Chem. 289, 26882–26894.
Bocci, V., 2012. How a calculated oxidative stress can yield multiple therapeutic effects. Free Radic. Res. 46, 1068–1075.
Bocci, V., Valacchi, G., 2015. Nrf2 activation as target to implement therapeutic treatments. Front. Chem. 3, 4.
Bogolyubov, D., Stepanova, I., Parfenov, V., 2009. Universal nuclear domains of somatic and germ cells: some lessons from oocyte interchromatin granule cluster and Cajal body structure and molecular composition. Bioessays 31, 400–409.
Bolstad, B.M., Irizarry, R.A., Astrand, M., Speed, T.P., 2003. A comparison of normalization methods for high density oligonucleotide array data based on variance and bias. Bioinformatics 19, 185–193.
Brigelius-Flohe, R., Flohe, L., 2011. Basic principles and emerging concepts in the redox control of transcription factors. Antioxid. Redox Signal. 15, 2335–2381.
Brouard, S., Otterbein, L.E., Anrather, J., Tobiasch, E., Bach, F.H., Choi, A.M., Soares, M.P., 2000. Carbon monoxide generated by heme oxygenase 1 suppresses endothelial cell apoptosis. J. Exp. Med. 192, 1015–1026.
Cisterna, B., Biggiogera, M., 2010. Ribosome biogenesis: from structure to dynamics. Int. Rev. Cell Mol. Biol. 284, 67–111.
Cmarko, D., Verschure, P.J., Martin, T.E., Dahmus, M.E., Krause, S., Fu, X.D., van Driel, R., Fakan, S., 1999. Ultrastructural analysis of transcription and splicing in the cell nucleus after bromo-UTP microinjection. Mol. Biol. Cell 10, 211–223.
Cmarko, D., Verschure, P.J., Rothblum, L.I., Hernandez-Verdun, D., Amalric, F., van Driel, R., Fakan, S., 2000. Ultrastructural analysis of nucleolar transcription in cells microinjected with 5-bromo-UTP. Histochem. Cell Biol. 113, 181–187.
Costanzo, M., Cisterna, B., Vella, A., Cestari, T., Covi, V., Tabaracci, G., Malatesta, M., 2015. Low ozone concentrations stimulate cytoskeletal organization, mitochondrial activity and nuclear transcription. Eur. J. Histochem. 59, 2515.
Davies, A., Pottage, T., Bennett, A., Walker, J., 2011. Gaseous and air decontamination technologies for *Clostridium difficile* in the healthcare environment. J. Hosp. Infect. 77, 199–203.
Elvis, A.M., Ekta, J.S., 2011. Ozone therapy: a clinical review. J. Nat. Sci. Biol. Med. 2, 66–70.
Fakan, S., 2004. Ultrastructural cytochemical analyses of nuclear functional architecture. Eur. J. Histochem. 48, 5–14.
Gingras, D., Bendayan, M., 1994. Compartmentalization of secretory proteins in pancreatic zymogen granules as revealed by immunolabeling on cryo-fixed and molecular distillation processed tissue. Biol. Cell. 81, 153–163.
Grochot-Przeczek, A., Dulak, J., Jozkowicz, A., 2013. Therapeutic angiogenesis for revascularization in peripheral artery disease. Gene 525, 220–228.
Güçlü, A., Erken, H.A., Erken, G., Dodurga, Y., Yay, A., Özçoban, Ö., Şimşek, H., Akçılar, A., Koçak, F.E., 2016. The effects of ozone therapy on caspase pathways, TNF-α, and HIF-1α in diabetic nephropathy. Int. Urol. Nephrol. 48, 441–450.
Gupta, G., Mansi, B., 2012. Ozone therapy in periodontics. J. Med. Life 5, 59–67.
Hayat, M.A., 1992. Quantitation of immunogold labelling. Micron Microsc. Acta 23, 1–16.
Huang, H.C., Nguyen, T., Pickett, C.B., 2000. Regulation of the antioxidant response element by protein kinase C-mediated phosphorylation of NF-E2-related factor 2. Proc. Natl. Acad. Sci. U. S. A. 97, 12475–12480.
Irizarry, R.A., Hobbs, B., Collin, F., Beazer-Barclay, Y.D., Antonellis, K.J., Scherf, U., Speed, T.P., 2003. Exploration, normalization, and summaries of high density oligonucleotide array probe level data. Biostatistics 4, 249–264.
Jensen, P.O., Larsen, J., Christiansen, J., Larsen, J.K., 1993. Flow cytometric measurement of RNA synthesis using bromouridine labelling and bromodeoxyuridine antibodies. Cytometry 14, 455–458.
Khalil, H.S., Goltsov, A., Langdon, S.P., Harrison, D.J., Bown, J., Deeni, Y., 2015. Quantitative analysis of NRF2 pathway reveals key elements of the regulatory circuits underlying antioxidant response and proliferation of ovarian cancer cells. J. Biotechnol. 202, 12–30.
Lafarga, M., Berciano, M.T., Andres, M.A., 1993. Protein-synthesis inhibition induces perichromatin granule accumulation and intranuclear rodlet formation in osmotically stimulated supraoptic neurons. Anat. Embryol. 187, 363–369.
Larini, A., Bianchi, L., Bocci, V., 2003. The ozone tolerance: (I) enhancement of antioxidant enzymes is ozone dose-dependent in Jurkat cells. Free Radic. Res. 37, 1163–1168.
Malatesta, M., Biggiogera, M., Cisterna, B., Balietti, M., Bertoni-Freddari, C., Fattoretti, P., 2010. Perichromatin fibrils accumulation in hepatocyte nuclei reveals alterations of pre-mRNA processing during ageing. DNA Cell Biol. 29, 49–57.
Molinari, F., Simonetti, V., Franzini, M., Pandolfi, S., Vaiano, F., Valdenassi, L., Liboni, W., 2014. Ozone autohemotherapy induces long-term cerebral metabolic changes in multiple sclerosis patients. Int. J. Immunopathol. Pharmacol. 27, 379–389.
Niki, E., 2016. Oxidative stress and antioxidants: distress or eustress? Arch. Biochem. Biophys. 595, 19–24.
Ozbay, I., Ital, I., Kucur, C., Akcılar, R., Deger, A., Aktas, S., Oghan, F., 2017. Effects of ozone therapy on facial nerve regeneration. Braz. J. Otorhinolaryngol. 83, 168–175.
Puvion, E., Puvion-Dutilleul, F., 1996. Ultrastructure of the nucleus in relation to transcription and splicing: roles of perichromatin fibrils and interchromatin granules. Exp. Cell Res. 229, 217–225.
Quesada, A., Ogi, J., Schultz, J., Handforth, A., 2011. C-terminal mechano-growth factor induces heme oxygenase-1-mediated neuroprotection of SH-SY5Y cells via the protein kinase Cc/Nrf2 pathway. J. Neurosci. Res. 89, 394–405.
Re, L., Mawsouf, M.N., Menéndez, S., León, O.S., Sánchez, G.M., Hernández, F., 2008. Ozone therapy: clinical and basic evidence of its therapeutic potential. Arch. Med. Res. 39, 17–26.
Re, L., Martínez-Sánchez, G., Bordicchia, M., Malcangi, G., Pocognoli, A., Morales-Segura, M.A., Rothchild, J., Rojas, A., 2014. Is ozone pre-conditioning effect linked to Nrf2/EpRE activation pathway in vivo? A preliminary result. Eur. J. Pharmacol. 742, 158–162.
Sagai, M., Bocci, V., 2011. Mechanisms of action involved in ozone therapy: is healing induced via a mild oxidative stress? Med. Gas Res. 1, 29.
Salem, N.A., Assaf, N., Ismail, M.F., Khadrawy, Y.A., Samy, M., 2016. Ozone therapy in ethidium bromide-induced demyelination in rats: possible protective effect. Cell. Mol. Neurobiol. 36, 943–954.
Schmittgen, T.D., Livak, K.J., 2008. Analyzing real-time PCR data by the comparative C(T) method. Nat. Protoc. 3, 1101–1108.
Schul, W., Groenhout, B., Koberna, K., Takagaki, Y., Jenny, A., Manders, E.M., Raska, I., van Driel, R., de Jong, L., 1996. The RNA 3′ cleavage factors CstF 64 kDa and CPSF 100 kDa are concentrated in nuclear domains closely associated with coiled bodies and newly synthesized RNA. EMBO J. 15, 2883–2892.
Schwarzacher, H.G., Wachtler, F., 1993. The nucleolus. Anat. Embryol. (Berl) 188, 515–536.
Sies, H., 2017. Hydrogen peroxide as a central redox signaling molecule in physiological oxidative stress: oxidative eustress. Redox Biol. 11, 613–619.
Sun, J., Hoshino, H., Takaku, K., Nakajima, O., Muto, A., Suzuki, H., Tashiro, S., Takahashi, S., Shibahara, S., Alam, J., Taketo, M.M., Yamamoto, M., Igarashi, K., 2002. Hemoprotein Bach1 regulates enhancer availability of heme oxygenase-1 gene. EMBO J. 21, 5216–5224.
Travagli, V., Zanardi, I., Valacchi, G., Bocci, V., 2010. Ozone and ozonated oils in skin diseases: a review. Mediat. Inflamm. 2010, 610418.
Tukey, J.W., 1977. Some thoughts on clinical trials, especially problems of multiplicity. Science 198, 679–684.
Tural Emon, S., Uslu, S., Ilgaz Aydinlar, E., Irban, A., Ince, U., Orakdogen, M., Gulec-Suyen, G., 2016. Effects of ozone on spinal cord recovery via Wnt/β-catenin pathway following spinal cord injury in rats. Turk. Neurosurg. http://dx.doi.org/10.5137/

1019-5149.JTN.17508-16.1.
Vandesompele, J., De Preter, K., Pattyn, F., Poppe, B., Van Roy, N., De Paepe, A., Speleman, F., 2002. Accurate normalization of real-time quantitative RT-PCR data by geometric averaging of multiple internal control genes. Genome Biol. 3 RESEARCH0034.
Zhang, J., Hung, A.C., Ng, P.Y., Nakayama, K., Hu, Y., Li, B., Porter, A.G., Dhakshinamoorthy, S., 2009. PKCdelta mediates Nrf2-dependent protection of neuronal cells from NO-induced apoptosis. Biochem. Biophys. Res. Commun. 386, 750–756.